J|A|C|S
ARTICLES

Tunable Bifunctional Silyl Ether Cross-Linkers for the Design of Acid-Sensitive Biomaterials

Matthew C. Parrott,[†,§,#] J. Chris Luft,[†,§,#] James D. Byrne,[†,§,#] John H. Fain,[†,§,#] Mary E. Napier,[†,§,#] and Joseph M. DeSimone*[,†,‡,§,∥,⊥,#,▽,○]

Departments of Chemistry and Pharmacology, Carolina Center of Cancer Nanotechnology Excellence, Institute for Advanced Materials, Institute for Nanomedicine, and Lineberger Comprehensive Cancer Center, University of North Carolina, Chapel Hill, North Carolina 27599, United States, Department of Chemical and Biomolecular Engineering, North Carolina State University, Raleigh, North Carolina 27695, United States, and Sloan-Kettering Institute for Cancer Research, Memorial Sloan-Kettering Cancer Center, New York, New York 10021, United States

Received September 22, 2010; E-mail: desimone@email.unc.edu

Abstract: Responsive polymeric biomaterials can be triggered to degrade using localized environments found in vivo. A limited number of biomaterials provide precise control over the rate of degradation and the release rate of entrapped cargo and yield a material that is intrinsically nontoxic. In this work, we designed nontoxic acid-sensitive biomaterials based on silyl ether chemistry. A host of silyl ether cross-linkers were synthesized and molded into relevant medical devices, including Trojan horse particles, sutures, and stents. The resulting devices were engineered to degrade under acidic conditions known to exist in tumor tissue, inflammatory tissue, and diseased cells. The implementation of silyl ether chemistry gave precise control over the rate of degradation and afforded devices that could degrade over the course of hours, days, weeks, or months, depending upon the steric bulk around the silicon atom. These novel materials could be useful for numerous biomedical applications, including drug delivery, tissue repair, and general surgery.

Introduction

Silyl ethers are among the most widely used protecting groups in organic chemistry.[1] Their popularity can be attributed to the fact that the rate of deprotection can be modulated by varying the substituents on the silicon atom. For instance, trimethylsilyl ether (TMS), triethylsilyl ether (TES), and triisopropylsilyl ether (TIPS) protecting groups have relative stabilities toward acid-catalyzed hydrolysis of 1, 64, and 700 000, respectively.[1] Simply by changing the substituents from methyl to ethyl to isopropyl, one can alter the rate of deprotection by orders of magnitude. Additionally, silyl ethers provide precise control over the rate of deprotection, the mechanism of deprotection, and the overall stability of a material. This class of chemistries has remained relatively unnoticed outside of protecting-group strategies. A successful adaptation of silyl ether chemistry, however, would afford a wide range of materials programmed to degrade under specific conditions found in vivo.

Researchers have exploited in vivo reducing environments,[2−4] enzymes,[5−7] and pH gradients[8−10] to trigger the cleavage or degradation of biomaterials. Specifically, hydrazones,[11] trityls,[12] aconityls,[13] vinyl ethers,[14] polyketals,[15,16] acetals,[17] poly(ortho esters),[18] and thiopropionates[19] utilize naturally occurring pH

† Department of Chemistry, University of North Carolina.
‡ Department of Pharmacology, Eshelman School of Pharmacy, University of North Carolina.
§ Carolina Center of Cancer Nanotechnology Excellence, University of North Carolina.
∥ Institute for Advanced Materials, University of North Carolina.
⊥ Institute for Nanomedicine, University of North Carolina.
Lineberger Comprehensive Cancer Center, University of North Carolina.
▽ North Carolina State University.
○ Sloan-Kettering Institute for Cancer Research.

(1) Wuts, P. G. M.; Greene, T. W. *Greene's Protective Groups in Organic Synthesis*, 4th ed.; Wiley: New York, 2007.
(2) Bellomo, G.; Vairetti, M.; Stivala, L.; Mirabelli, F.; Richelmi, P.; Orrenius, S. *Proc. Natl. Acad. Sci. U.S.A.* **1992**, *89*, 4412–4416.
(3) Jones, D. P.; Carlson, J. L.; Mody, V. C.; Cai, J. Y.; Lynn, M. J.; Sternberg, P. *Free Radical Biol. Med.* **2000**, *28*, 625–635.
(4) Meister, A. *Pharmacol. Ther.* **1991**, *51*, 155–194.
(5) Chau, Y.; Tan, F. E.; Langer, R. *Bioconjugate Chem.* **2004**, *15*, 931–941.
(6) Mohamed, M. M.; Sloane, B. F. *Nat. Rev. Cancer* **2006**, *6*, 764–775.
(7) Romberg, B.; Hennink, W. E.; Storm, G. *Pharm. Res.* **2008**, *25*, 55–71.
(8) Helmlinger, G.; Schell, A.; Dellian, M.; Forbes, N. S.; Jain, R. K. *Clin. Cancer Res.* **2002**, *8*, 1284–1291.
(9) Mellman, I.; Fuchs, R.; Helenius, A. *Annu. Rev. Biochem.* **1986**, *55*, 663–700.
(10) Sun-Wada, G. H.; Wada, Y.; Futai, M. *Cell Struct. Funct.* **2003**, *28*, 455–463.
(11) Di Stefano, G.; Lanza, M.; Kratz, F.; Merina, L.; Fiume, L. *Eur. J. Pharm. Sci.* **2004**, *23*, 393–397.
(12) Patel, V. F.; Hardin, J. N.; Mastro, J. M.; Law, K. L.; Zimmermann, J. L.; Ehlhardt, W. J.; Woodland, J. M.; Starling, J. J. *Bioconjugate Chem.* **1996**, *7*, 497–510.
(13) Shen, W. C.; Ryser, H. J. P. *Biochem. Biophys. Res. Commun.* **1981**, *102*, 1048–1054.
(14) Shin, J.; Shum, P.; Thompson, D. H. *J. Controlled Release* **2003**, *91*, 187–200.
(15) Heffernan, M. J.; Murthy, N. *Bioconjugate Chem.* **2005**, *16*, 1340–1342.
(16) Sankaranarayanan, J.; Mahmoud, E. A.; Kim, G.; Morachis, J. M.; Almutairi, A. *ACS Nano* **2010**, *4*, 5930–5936.
(17) Gillies, E. R.; Fréchet, J. M. J. *Bioconjugate Chem.* **2005**, *16*, 361–368.

Scheme 1. Synthesis of Bifunctional Silyl Ether (BSE) Cross-Linkers

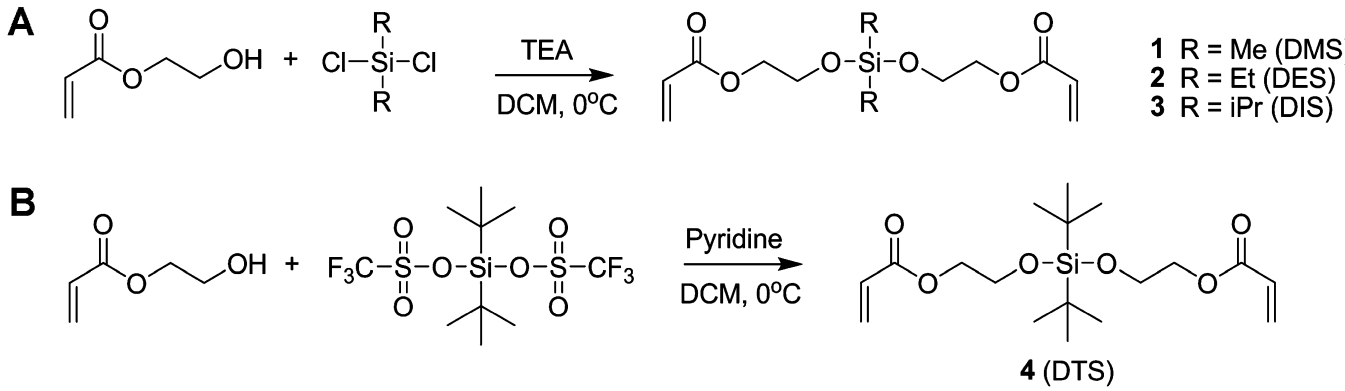

gradients to catalyze degradation, but they are limited by poor tunability, toxic byproducts, or meticulous, multistep syntheses. Conversely, a silyl ether linkage can be formed in one simple step, gives nontoxic byproducts upon degradation, and can be designed to degrade at different rates merely by altering the substituent on the silicon atom.

One type of silyl ether linkage that is of interest is the bifunctional silyl ether (BSE). BSEs consist of a C−O−Si(R)$_2$−O−C linkage and are commonly used for the protection of 1,2- and 1,3-diols.[20−22] The less-hindered dimethyl, diethyl, and diisopropyl BSEs are exceedingly susceptible to acid-catalyzed hydrolysis and are typically avoided as protecting groups. Although this property is unfavorable for protection strategies, less-hindered BSEs provide the ideal characteristics for highly susceptible, acid-sensitive biomaterials.

Results and Discussion

We therefore set out to prepare a collection of BSE cross-linkers with a variety of substituents on the silicon atom. The production of the desired cross-linkers utilized commercially available starting materials and required only one synthetic step, which proved to be inexpensive, rapid, and facile. Two similar silyl ether reactions (Scheme 1A,B) provided four novel, photopolymerizable cross-linkers denoted as **1**, **2**, **3**, and **4**. For simplicity, we refer to the different cross-linkers according to the substituents on the silicon atom. For example, cross-linker **1** with two methyl substituents is called dimethylsilyl ether or DMS, and cross-linker **2** with two ethyl substituents is called diethylsilyl ether or DES.

Each cross-linker was molded into "Trojan horse" microparticles using a particle fabrication process called *p*article *r*eplication *i*n *n*onwetting *t*emplates (PRINT).[23] PRINT is a top-down approach used to manufacture microparticles[24−26] and nanoparticles[27−29] with well-defined sizes and shapes. Two particle shapes were fabricated: 5 μm cube particles (Figure 1A,B) and 3 μm hexnut particles (Figure 1C,D) (full particle characterization can be found in the Supporting Information). The microparticles were successfully prepared with each BSE cross-linker and were degraded under acidic conditions known to exist inside various cellular compartments.[9] The larger 5 μm cube particles were employed to determine the rate of particle degradation at simulated lysosomal, endosomal, and physiological pH (pH 5.0, 6.0, and 7.4, respectively).[9] A quantitative analysis of particle degradation was carried out on particles fabricated from DMS (**1**), DES (**2**), and diisopropylsilyl (DIS) (**3**) cross-linkers and loaded with 2 wt % rhodamine B. The particles were degraded, and aliquots of the supernatant were removed and filtered; the concentrations of rhodamine B were then measured using UV spectroscopy. For accuracy, this experiment was repeated three times, and the average data were fit to an exponential growth model to determine the degradation half-lives.

A plot of rhodamine B release versus time for particles fabricated with the DMS cross-linker (Figure 2A) displayed an accelerated rate of degradation when dispersed in a medium buffered at pH 5.0 and exhibited a degradation half-life of 0.091 days or 2.19 h (Table 1). The same particles dispersed in a medium buffered at pH 6.0 had a half-life of 1.08 days, and particles dispersed in a medium buffered at pH 7.4 had a half-life of 2.94 days. From these data it was apparent that the particles fabricated from the DMS cross-linker preferentially degraded under acidic conditions and that the rate of degradation was accelerated as the pH decreased. Under identical conditions, particles fabricated with the DES cross-linker also degraded preferentially under acidic conditions (Figure 2B), but the rate of degradation was noticeably different. The DES particles appeared to degrade 13.6 times slower than the DMS particles when dispersed in a medium buffered at pH 5.0 and ~10 times slower when degraded in media buffered at pH 6.0 or 7.4. Furthermore, the degradation of particles fabricated with the DIS cross-linker (Figure 2C) was slower by 2 orders of magnitude at all pH values. This illustrates that simply by changing the substituent around the silicon atom one can effectively modulate the rate of particle degradation from hours to days to weeks to months.

Intracellular degradation of silyl ether PRINT particles could be visualized using transmission electron microscopy (TEM)

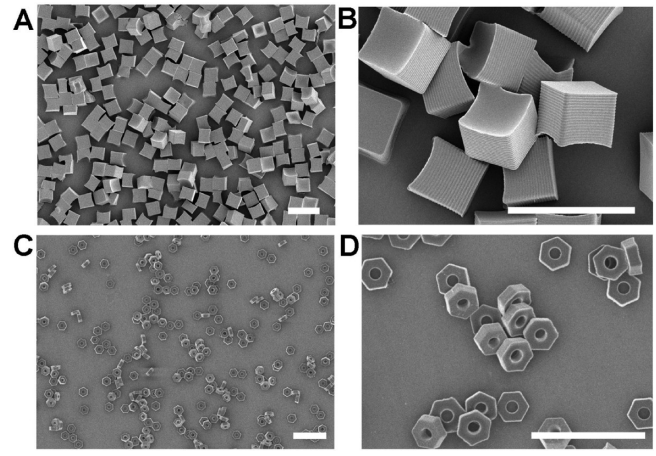

Figure 1. Scanning electron micrographs of (A, B) 5 μm cubes and (C, D) 3 μm hexnut particles fabricated using PRINT (scale bars: 10 μm).

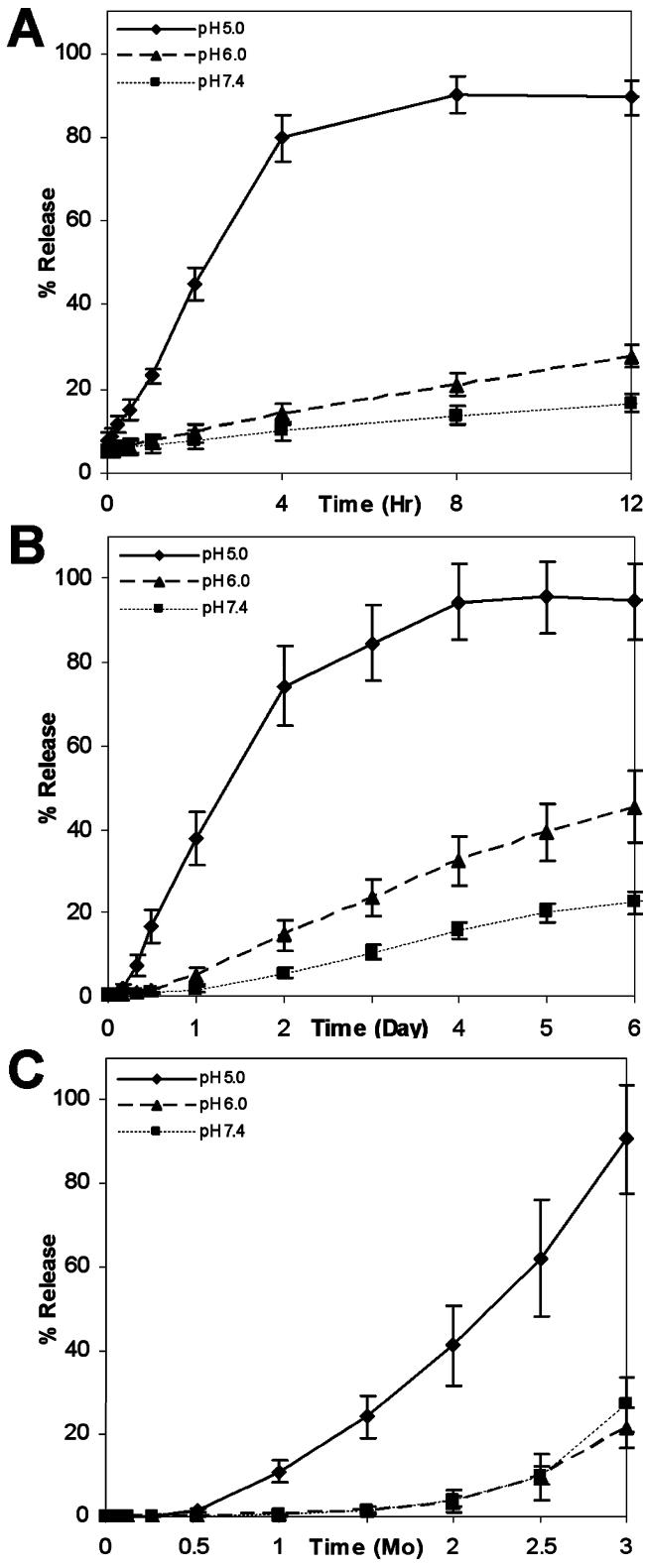

Figure 2. Percent rhodamine-B release vs time for 5 μm cube particles fabricated from (A) DMS, (B) DES, and (C) DIS cross-linkers.

and laser scanning confocal microscopy. We selected the hexnut-shaped particles for this experiment because of their unique shape, which makes them easily distinguishable from cellular compartments. Two separate batches of hexnut particles were fabricated, one from the rapidly degrading DMS cross-linker and the other from the nondegrading di-*tert*-butylsilyl (DTS) cross-linker. A small amount of positively charged *N*-(3-aminopropyl)methacrylamide hydrochloride (APMA-HCl) was added to the composition to ensure a positive ζ potential and cellular internalization.[30] The TEM micrographs were captured in bright-field mode, in which low-density material appears white and high-density material appears dark.[31] Particles fabricated with the rapidly degrading DMS cross-linker can be seen in Figure 3A, in which one DMS hexnut particle was internalized and three DMS-hexnut particles remained outside the HeLa cell. A closer look at the internalized particle (Figure 3B) showed a bright white mass resembling a hexnut particle. The bright white color signifies that the particle became less dense than the surrounding intracellular matrix and significantly less dense than the same particles found outside the cell. The noninternalized DMS hexnut particles (Figure 3C) appeared to be completely intact, and the size and shape of the particles were found to be equivalent to those of the particles imaged by scanning electron microscopy. Additional micrographs were taken to monitor the course of the DMS hexnut degradation, and the internalized hexnut particles always became less dense (bright white) and appeared to swell (Figure 3D), then fragment (Figure 3E), and finally undergo surface erosion (Figure 3F). Particles prepared with the nondegrading DTS cross-linker can be seen in Figure 3G,H. These particles were also internalized within HeLa cells (and hence exposed to an acidic environment) but because of the stability of the cross-linker, the particles were not susceptible to degradation. In addition, there was no noticeable change in the shape, size, or density of the DTS hexnut particles internalized inside HeLa cells.

Table 1. Degradation Half-Lives ($t_{1/2}$) and Normalized Stabilities of 5 μm Silyl Ether Particles

	DMS			DES			DIS		
pH	5.0	6.0	7.4	5.0	6.0	7.4	5.0	6.0	7.4
$t_{1/2}$ (day)[a]	0.091	1.08	2.94	1.24	8.98	28.0	30.7	110	110
norm. stab.[b]	1.00	11.8	32.3	13.6	98.7	308	337	1209	1209

[a] Degradation data were imported into Origin and fit to an exponential growth curve. All R^2 values were greater than 0.99. [b] Relative to DMS at pH 5.0.

(18) Toncheva, V.; Schacht, E.; Ng, S. Y.; Barr, J.; Heller, J. *J. Drug Targeting* **2003**, *11*, 345–353.
(19) Oishi, M.; Nagasaki, Y.; Itaka, K.; Nishiyama, N.; Kataoka, K. *J. Am. Chem. Soc.* **2005**, *127*, 1624–1625.
(20) Furusawa, K.; Katsura, T. *Tetrahedron Lett.* **1985**, *26*, 887–890.
(21) Kumagai, D.; Miyazaki, M.; Nishimura, S. I. *Tetrahedron Lett.* **2001**, *42*, 1953–1956.
(22) Trost, B. M.; Caldwell, C. G. *Tetrahedron Lett.* **1981**, *22*, 4999–5002.
(23) Rolland, J. P.; Maynor, B. W.; Euliss, L. E.; Exner, A. E.; Denison, G. M.; DeSimone, J. M. *J. Am. Chem. Soc.* **2005**, *127*, 10096–10100.
(24) Brown, E.; Forman, N. A.; Orellana, C. S.; Zhang, H. J.; Maynor, B. W.; Betts, D. E.; DeSimone, J. M.; Jaeger, H. M. *Nat. Mater.* **2010**, *9*, 220–224.
(25) Herlihy, K. P.; Nunes, J.; DeSimone, J. M. *Langmuir* **2008**, *24*, 8421–8426.
(26) Nunes, J.; Herlihy, K. P.; Mair, L.; Superfine, R.; DeSimone, J. M. *Nano Lett.* **2010**, *10*, 1113–1119.
(27) Gratton, S. E. A.; Ropp, P. A.; Pohlhaus, P. D.; Luft, J. C.; Madden, V. J.; Napier, M. E.; DeSimone, J. M. *Proc. Natl. Acad. Sci. U.S.A.* **2008**, *105*, 11613–11618.
(28) Kelly, J. Y.; DeSimone, J. M. *J. Am. Chem. Soc.* **2008**, *130*, 5438–5439.
(29) Petros, R. A.; Ropp, P. A.; DeSimone, J. M. *J. Am. Chem. Soc.* **2008**, *130*, 5008–5009.
(30) Miller, C. R.; Bondurant, B.; McLean, S. D.; McGovern, K. A.; O'Brien, D. F. *Biochemistry* **1998**, *37*, 12875–12883.
(31) Fultz, B.; Howe, J. M. *Transmission Electron Microscopy and Diffractometry of Materials*, 3rd ed.; Springer: New York, 2008.

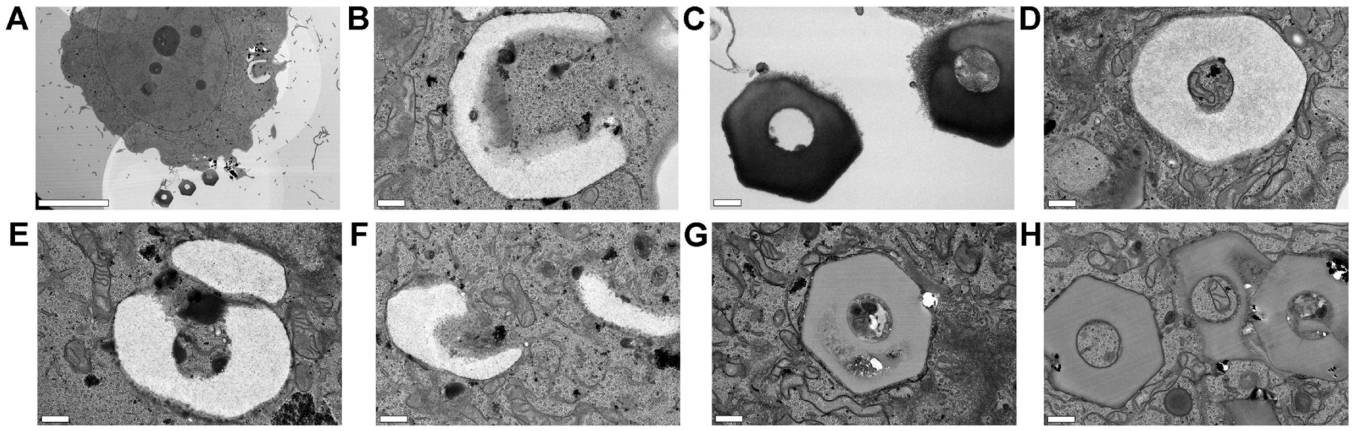

Figure 3. TEM micrographs of PRINT hexnut particles incubated in HeLa cells: (A−F) rapidly degrading hexnut particles fabricated from the DMS cross-linker [scale bars: (A) 10 μm; (B−F) 0.5 μm]; (G, H) nondegrading hexnut particles fabricated from the DTS cross-linker (scale bars: 0.5 μm).

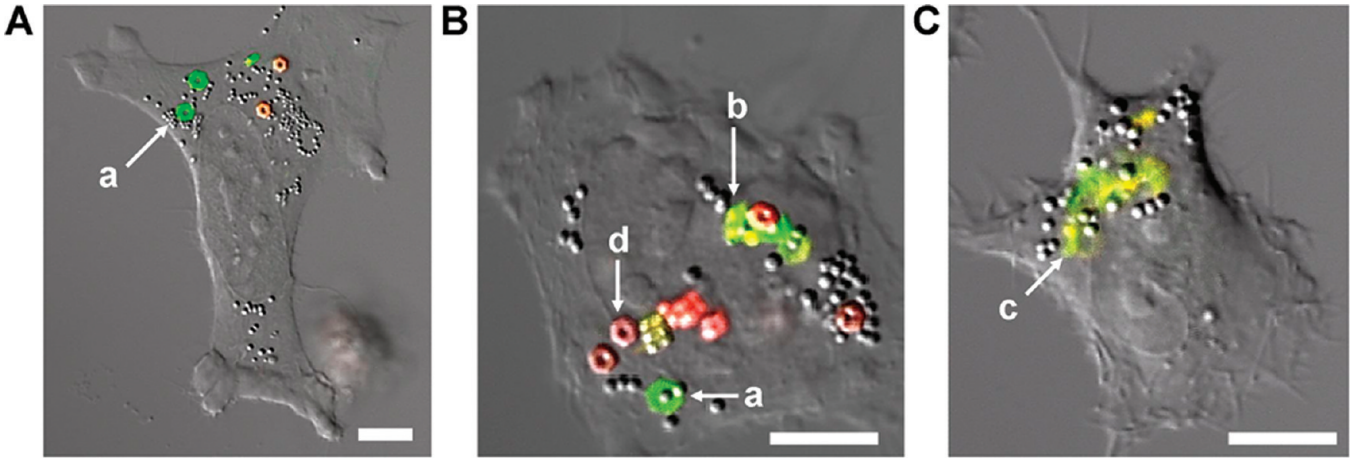

Figure 4. Laser scanning confocal micrographs of HeLa cells incubated with rapidly degrading hexnut particles (green) and nondegrading hexnut particles (red). The micrographs highlight the phases of particle degradation: (a) swelling, (b) fragmentation, and (c) complete degradation. The nondegradable particles (d) showed no change when exposed to intracellular conditions. (Scale bars: 10 μm.)

Further investigation of intracellular degradation of silyl ether particles was achieved utilizing laser scanning confocal microscopy. Two particle types were fabricated, one containing the rapidly degrading DMS cross-linker with fluorescein *o*-acrylate (a green fluorescent dye) and the other containing the nondegrading DTS cross-linker and methacryloxyethyl thiocarbamoyl rhodamine B (a red fluorescent dye). HeLa cells were incubated for 24 h with both the rapidly degrading particles (green) and the nondegrading particles (red) (Figure 4). It was clear that after cellular internalization, the nondegrading DTS particles appeared to maintain the same size and shape and were not altered by intercellular conditions. On the other hand, the degradable DMS particles exhibited a number of different characteristics, including enlargement or swelling, loss of the distinct hexnut shape, fragmentation, and complete degradation, as illustrated by the diffuse green fluorescence found in Figure 4C.

Cell viability experiments were performed to determine whether the degradation byproducts were toxic. This was accomplished by separately dosing all four silyl-ether hexnut particles (DMS, DES, DIS, and DTS) onto both HeLa and SKOV3 cell lines. The cytotoxicity of each particle was determined using the CellTiter-Glo luminescent cell viability assay (Figure 5). All of the silyl ether PRINT particles dosed onto HeLa and SKOV3 cells showed minimal toxicity across a large concentration range. These assays suggest that the silyl ether chemistry is nontoxic and that the degradation byproducts appear to be well-tolerated in cells.

The novelty of BSE cross-linkers is not limited to particle-based drug delivery applications. Devices fabricated from silyl ether biomaterials could also be useful for tissue repair and general surgery. Biodegradable and bioabsorbable devices are routinely used in hospitals and are often made from a copolymer of lactic acid and glycolic acid identified as poly(lactic-*co*-glycolic acid) or PLGA.[32] A device made from PLGA is susceptible to both acid-catalyzed degradation and enzymatic degradation by esterases.[33−35] As a result of variable levels of enzymes, PLGA can degrade at different rates in different patients.[36] To the best of our knowledge, an enzyme specific to the silyl ether linkage does not exist. Therefore, devices fabricated from silyl ether biomaterials should be susceptible only to an acid-catalysis mechanism and consequently minimize patient-to-patient variability.

Rudimentary medical devices such as sutures and stents were manufactured from the silyl ether cross-linkers according to

(32) Jagur-Grodzinski, J. *Polym. Adv. Technol.* **2006**, *17*, 395–418.
(33) Chu, C. C.; Williams, D. F. *J. Biomed. Mater. Res.* **1983**, *17*, 1029–1040.
(34) Parviainen, M.; Sand, J.; Harmoinen, A.; Kainulainen, H.; Valimaa, T.; Tormala, P.; Nordback, I. *Pancreas* **2000**, *21*, 14–21.
(35) Williams, D. F.; Mort, E. *J. Bioeng.* **1977**, *1*, 231.
(36) Davis, M. E. Private communication.

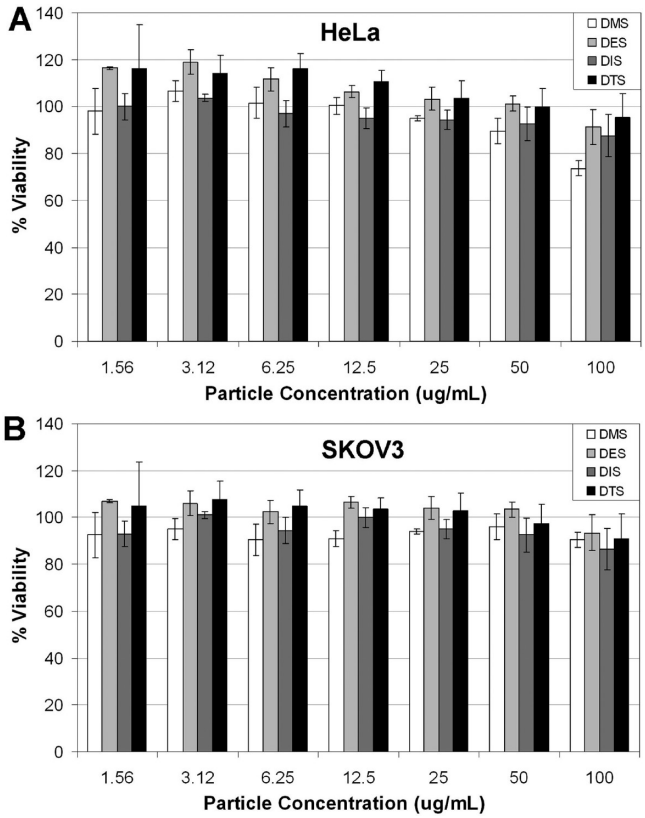

Figure 5. Cell viability assay (CellTiter-Glo) of hexnut particles fabricated from DMS, DES, DIS and DTS cross-linkers. The assay was performed using (A) HeLa and (B) SKOV3 cells.

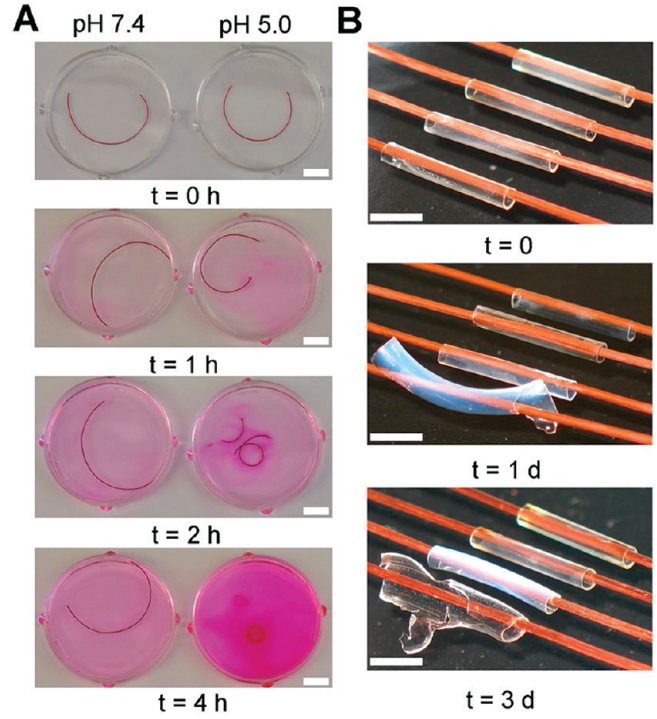

Figure 6. Biomedical devices fabricated from silyl ether cross-linkers. (A) Silyl ether sutures fabricated from DMS and rhodamine B were degraded in media buffered at pH 7.4 and 5.0 (scale bars: 1 cm). (B) Silyl ether stents fabricated from (left to right) compounds **1**−**4** were placed in a medium buffered at pH 5.0 and allowed to degrade (scale bars: 1 cm).

several different procedures. As shown in Figure 6A, a thin fiber of the DMS cross-linker was prepared with a small amount of rhodamine B. The fiber was designed with a diameter of 0.3 mm and a length of 50 cm and would be recognized as a class 2-0 USP suture. The fiber was cut and placed in media buffered at pH 5.0 and 7.4. Analogous to the PRINT particles, the rate of degradation of the DMS fiber was accelerated at pH 5.0. Furthermore, the fiber suspended in the medium buffered at pH 7.4 remained unbroken and showed minimal release of the rhodamine B cargo over the course of 4 h.

Stent-like devices were also made using each silyl ether cross-linker (Figure 6B). Each stent had an outer diameter of 3 mm, an inner diameter of 2.5 mm, a thickness of 0.25 mm, and a length of 25 mm, analogous to the dimensions of a typical coronary stent. Each stent was placed in an acidic solution (pH 5.0) and allowed to degrade over the course of 3 days. After the experiment was complete, the stent made from the rapidly degrading DMS cross-linker showed significant changes in shape and morphology. The stent made from the DES cross-linker became swollen and opaque, indicating the onset of degradation, while the remaining DIS and DTS stents showed no change over the course of the experiment.

Conclusions

Bifunctional silyl ether cross-linkers were investigated as new biomedical materials useful for drug delivery and degradable devices. Using one facile synthetic step, we were able to synthesize four cross-linkers from commercially available reagents. Each cross-linker was successfully integrated into the PRINT platform and yielded Trojan horse particles for drug delivery. The particles were degraded in three different pH environments, and the rate of degradation was accelerated as the pH decreased. Interestingly, the rate of acid-catalyzed hydrolysis could be altered by orders of magnitude simply by changing the substituents on the silicon atom. In vitro particle degradation was visualized using TEM and laser scanning confocal spectroscopy, which highlighted preferential degradation of particles internalized inside cells. Preliminary in vitro cytotoxicity data suggested that these materials are well-tolerated across a large concentration range in two cell lines. Furthermore, the silyl ether biomaterials were molded into two practical medical devices and shown to preferentially degrade under reduced pH. The rational design and implementation of silyl ether chemistry has provided a fast and simple approach to a host of acid-sensitive biomaterials. Further development of this silyl ether chemistry could generate numerous devices susceptible to acidic environments, which could be useful in a vast number of applications.

Acknowledgment. The research was supported by National Institutes of Health Grants 1R01EB009565-02, U54CA119373 (Carolina Center of Cancer Nanotechnology), and 1DP10D006432-01 (NIH Pioneer Award); the University Cancer Research Fund at the University of North Carolina at Chapel Hill; the William R. Kenan Professorship at the University of North Carolina at Chapel Hill; and a sponsored research agreement with Liquidia Technologies. We also acknowledge Prof. Mark E. Davis for his helpful advice and discussions.

Supporting Information Available: Experimental details. This material is available free of charge via the Internet at http://pubs.acs.org.

JA108568G